An Effective Method for Studying Intermolecular Interactions in Binary Liquids with Hydrogen Bonds; FTIR Spectra and *Ab Initio* Calculations in the *N*-Methylformamide−Methanol System

Ewa Kamieńska-Piotrowicz,* Kamila Dziewulska, and Janusz Stangret

Department of Physical Chemistry, Chemical Faculty, Gdańsk University of Technology, Narutowicza 11/12, 80-233 Gdańsk, Poland

Received: December 4, 2009; Revised Manuscript Received: March 17, 2010

Molecular complexes in methanol (MeOH)−*N*-methylformamide (NMF) mixtures were studied based on their FTIR-ATR spectra, to which two methods of analysis were applied: factor analysis and a quantitative version of the difference-spectra method. The mean composition of a complex between NMF and MeOH molecules over the whole range of mixture compositions was determined. Absorbing species differentiated with regard to the interaction energies of the carbonyl oxygen with methanol molecules were recognized in both compositional regions with a marked excess of one component. Possible structures for complexes of various stoichiometries were optimized by *ab initio* calculations in the gas phase and both liquid NMF and MeOH using the polarizable continuum model (PCM). Thermodynamic functions calculated for the optimized structures were used to find the most stable structure for each stoichiometry. Individuals distinguished by the spectral analysis were assigned to the complexes of definite composition, and a linear correlation between the positions of the carbonyl group absorption and the total interaction energies of the complexes was found. The results of the spectral analysis of the NMF−MeOH mixtures were compared to those we obtained previously for similar binary systems, i.e., mixtures of methanol and formamide (FA) or *N*,*N*-dimethylformamide (DMF). It was shown that the factor analysis applied to the infrared spectra is an effective method for distinguishing molecular complexes with different polarizations of component molecules and allows for the detection of even weak intermolecular interactions and low-concentration species. Combined with the difference-spectra method, factor analysis provides a comprehensive picture of intermolecular interactions in binary mixtures.

Introduction

The characterization of intermolecular interactions is a crucial point in the understanding of liquid phases and hence of great interest in different areas of research such as chemistry, biochemistry, and biology. Among a variety of interactions, the importance of hydrogen bonds in biological systems and living organisms cannot be overestimated. The direct investigation of such systems is difficult because of their complexity and the many overlapping effects. Therefore, studies of simple compounds that can serve as models for biologically active ones are commonly undertaken. Binary mixtures of lower amides with methanol are suitable model subjects because the amide group is the basic unit of the peptide linkage and examining its interactions with methanol molecules may contribute to an explanation of the effects of alcohols on the stability of proteins. The essential task in the studies of model systems is to elaborate a methodology that actually increases knowledge about their structure. In this work, we offer an effective method for studying intermolecular interactions using a combination of experimental and computational methods to create a powerful tool for solving the above problem.

The main interactions in binary mixtures of methanol (MeOH) and formamide (FA) and its N-substituted methyl derivatives, *N*-methylformamide (NMF) and *N*,*N*-dimethylformamide (DMF), are hydrogen bonding between molecules of different components as well as between molecules of the same kind. Vibrational spectroscopy is the most convenient and appropriate method for studying hydrogen bonds because of the sensitivity of the spectra obtained to the molecular environment. In our previous studies of DMF−MeOH and FA−MeOH mixtures,[1,2] FTIR spectra were analyzed by two advanced methods: factor analysis, in the version written by Malinowski,[3] and a quantitative version of the difference-spectra method, described by one of the present authors.[4] As a result, the mean compositions of the complexes were obtained, as distinguished by the factor analysis, depending on the mixed solvent composition and the number of absorbing species differentiated with respect to their energetic states.

On the basis of the above information, we were able to propose only a general scheme for hydrogen bonding in complexes that would best explain the spectral results. Although this task was relatively simple in the first system, it was more difficult to resolve in the latter one because of its higher degree of complexity. In NMF−MeOH mixtures, additional difficulties due to the *cis*−*trans* isomerism of the NMF molecule were expected. Therefore, *ab initio* quantum-mechanical calculations of molecular complexes in this system were performed to support the interpretation of the spectral results. The geometries were calculated for isolated clusters (in the gas phase) as well as for complexes placed in the solvent treated as the continuous solvating medium using the polarizable continuum model (PCM). Thermodynamic functions obtained for the optimized structures were used to calculate the interaction energies of the clusters and their relative stabilities. Computational results for

* To whom correspondence should be addressed. Phone: +48 58 347 2593. Fax: +48 58 347 2694. E-mail: kamien@chem.pg.gda.pl.

10.1021/jp911530d
Published on Web 04/09/2010

the complexes in the liquid phase were compared with the spectral results and discussed together.

Although a growing interest in *N*-methylformamide has recently been observed,[5–12] the reports concerning NMF−MeOH mixtures date mainly from the previous decade. Excess enthalpies, which are positive over the whole range of system composition, show that the self-association of both components outweighs their ability for heteroassociation.[13] Other thermodynamic studies comprise excess volumes and excess Gibbs free energies at different temperatures.[14–16] These data have been analyzed using the Kirkwood−Buff theory of solutions to investigate solvation of *N*-methylformamide by methanol.[17,18] The existence of stable complexes in binary mixtures of *trans*-NMF and *cis*-NMF with methanol was confirmed by molecular-dynamics calculations.[18] Solvation of the NMF molecule through the carbonyl group in a dilute solution of methanol has been studied on the basis of the infrared shift of the ν(C−O) band and the NMR shift for the ^{13}C=O carbon.[19] The results suggested that the CO group can interact by hydrogen bonding with one or two methanol molecules. The effect of methanol as a solvent on the NMR ^{17}O isotropic shielding for *N*-methylformamide has been measured[20] and computed by different methods.[21–23] The geometry of the $(NMF)_1(MeOH)_1$ cluster in methanol has been optimized using a PCM approximation.[23]

This work provides a comprehensive study of the intermolecular interactions and structure of NMF−MeOH liquid mixtures over the whole range of their compositions, realized by a combination of experimental and theoretical methods. The usefulness of quantitative analysis for the infrared spectra of binary mixtures of amides (FA, NMF, DMF) with methanol was discussed and tested by confrontation with *ab initio* calculations performed for NMF−MeOH clusters at different ratios of components and various geometries.

Experimental Section

Chemicals and Measurements. Methanol (Aldrich, HPLC grade, 99.9+%) and *N*-methylformamide (Fluka, p.a., > 99%) were stored over 3 Å thermally activated molecular sieves (Aldrich) in a drybox. The solvents were then distilled prior to use with a Vigreux column, *N*-methylformamide under reduced pressure.

Mixtures of methanol and *N*-methylformamide were prepared by weighing to yield methanol mole fractions varying by ~0.025 in the ranges $0 \le x_{MeOH} \le 0.2$ and $0.8 \le x_{MeOH} \le 1$ and by ~0.05 in the remaining range. The densities were measured using an Anton Paar DMA 5000 densimeter at 25.0 ± 0.001 °C. Both the compositions of the mixtures and their densities were determined to an accuracy of 10^{-5}.

FTIR spectra were recorded on a Nicolet 8700 spectrometer (Thermo Electron Co) employing an ATR technique using an HATR Specac Gateway accessory (six bounces) with a 550 μm thermostabilized flow through the top-plate-type assembly equipped with a germanium crystal (45°). The chamber of the apparatus was flushed with dry nitrogen before and during recording to remove atmospheric carbon dioxide and water vapor, which could contaminate the spectra. The data were collected from 128 scans with a 4 cm^{-1} resolution. The temperature was kept at 25.0 ± 0.1 °C by circulating thermostatic water and monitored by a thermocouple inside the cell.

ATR spectra were processed using the OMNIC 6.2 software with the advanced ATR correction. It accounts for several factors influencing the ATR spectra, e.g., the dependence of the sample penetration depth by the infrared beam on wavenumber and the shift of bands to lower wavenumbers caused by dispersion of the refractive index and the deviation from Beer's law caused by nonpolarization effects. The refractive index of the mixtures, needed for applying the ATR correction, was measured using an SL6 (Poland) refractometer at 25.0 ± 0.1 °C.

Residual contributions from carbon dioxide and water vapor in the spectra were compensated for by the Thermo Nicolet software or by subtracting the separately recorded atmospheric gas spectrum. All spectra were baseline corrected before analysis.

Analysis of Spectral Data. The difference-spectra method applied to the spectra of binary liquid mixtures leads to the extraction of the spectrum of a component in excess (solvent) affected by the other component (solute). The solute should not absorb in the considered range of the spectrum. The method is based on the assumption that the spectrum of a solution, ε, is the sum of the spectrum of the bulk solvent (identical with that of the pure solvent), ε_b, and of the solute-affected spectrum of the solvent, ε_a. The latter can be calculated for each wavenumber from eq 1, as described by Stangret et al.:[24]

$$\varepsilon_a = \frac{1}{NM}\left(\frac{\partial \varepsilon}{\partial m}\right)_{m=0} + \varepsilon_b \quad (1)$$

where M is the molecular weight of the solvent (kg mol^{-1}), N is the affected number (denoting the number of solvent molecules influenced by one molecule of solute), and m is the molality of the solution (mol kg^{-1}). The parameter N is not equivalent with the solvation number determined by other techniques, especially when the affected spectrum does not differ distinctly from the bulk spectrum. For a discussion of this matter, see ref 24.

The derivative $\partial\varepsilon/\partial m$ at zero molality is obtained by an approximation of the ε value vs molality at each wavenumber using linear or quadratic regression. The trial affected spectra for different values of N are constructed using eq 1; the spectra are then approximated by a small number of analytical bands, both bulk spectrum and linear baseline. The affected number corresponds to the maximum value of N for which the contribution of the bulk spectrum in the affected spectrum decreases below 0.5%; this spectrum is treated as the "true" affected spectrum. Details of the computational procedure are described in ref 25. The method has been well tested in the solvation studies of both ionic[26–29] and nonionic[30–32] species.

The spectra were handled and analyzed using the commercial PC programs GRAMS/32 (Galactic Industries Corporation, Salem) and RAZOR (Spectrum Square Associates, Ithaca), run under GRAMS/32.

The factor analysis was performed using the commercial computer program Factor Analysis Toolbox for MATLAB (Applied Chemometrics Inc., Sharon). The spectral data were assembled into absorbances at given wavenumbers in methanol mole-fraction matrices. The main application used in this study was window factor analysis (WFA), which involves the extraction of the concentration profiles of the individual chemical species responsible for spectral data (factors). The essential feature of this method is that each profile is extracted independently and, moreover, without requiring any model of the system. The region of existence of the particular factor along the composition axis, the "window", is located by using an automatic window factor-analysis algorithm (AUTOWFA). The results of WFA analysis depend on the number of factors used in the computations. The correct number of factors is obtained by using the principal factor analysis algorithm (PFA), which

reproduces the spectral data and compares them with the experimental ones. When the "true" number of factors is used, this procedure generates a difference between the experimental and calculated spectral data comparable in intensity to the experimental noise level.

The method was originally tested by Zhao and Malinowski for $H_2O-MeOH$ mixtures[33] and applied previously by us for DMF−MeOH and FA−MeOH mixtures.[1,2]

Computational Details. *Ab initio* calculations were performed with the Gaussian 03 system[34] for the possible geometries of $(NMF)_n(MeOH)_m$ complexes, where $n = 1-2$, $m = 1-4$, and *cis* as well as *trans* isomers of NMF were considered. Initial structures of the complexes were constructed using the Hyperchem 6.0 PC program (Hypercube, Inc., Gainesville, FL). The structures were optimized in the framework of density functional theory (DFT) with the use of the B3LYP exchange-correlation functional and the standard Pople basis set 6-311++G(d,p). The Berny algorithm with *Tight* convergence criteria was applied. Numerical integrations were performed using an *UltraFine* grid consisting of 99 shells per atom and 590 points per shell. The GDIIS method was applied to speed up the optimization process.

The isolated structures were subsequently optimized in the liquid phase using the standard polarizable continuum model (PCM) in the self-consistent reaction field (SCRF) approach. The external solvent fields of pure NMF and pure MeOH were characterized by their respective dielectric constants. The maximum number of molecules in a cluster containing an NMF molecule that could be optimized in a solvent cavity was four.

The Gaussian output from the vibrational analysis for the optimized structures included their thermochemical characteristics: zero-point electronic energies, entropies and thermal corrections to energy, enthalpy, and Gibbs free energy.

Hyperchem 6.0 PC and GaussView 3.0 (Gaussian, Inc., Wallingford, CT) were used as tools for visualization of the results.

Results and Discussion

Spectral Results. The FTIR spectra of NMF−MeOH mixtures, measured over the whole range of compositions within wavenumbers of 4000−700 cm^{-1} are presented as an absorbance scale in Figure 1a; the region of the ν(O−H), ν(N−H), and ν(C−H) bands is enlarged in Figure 1b. Factor analysis was performed for the whole spectrum and, independently, for the carbonyl-group region. The hydroxyl-group region was not selected for a separate analysis because of the coincidence of the ν(O−H) band with other bands. For the same reason, the difference-spectra method was applied only to the ν(C−O) band of the amide treated as the solvent and not to the ν(O−H) band of methanol. The carbonyl-group absorption region, converted into the molar absorbance of NMF, is shown in Figure 1c.

From the factor analysis applied to the spectra over the whole range of wavenumbers, concentration profiles of the absorbing species were obtained (Figure 2a). Two of these, with maxima at the pure components, must correspond to the bulk NMF and bulk MeOH, respectively. The third one represents an intermolecular complex between components, with a maximum concentration at $x_{MeOH} \approx 0.64$. On the basis of the above, the molar concentrations of individual species were calculated and are shown in Figure 2b. The molar concentrations of complexed NMF and MeOH were subsequently used to calculate the ratio of MeOH and NMF molecules in the complex depending on the methanol mole fraction in the mixtures (Figure 3).

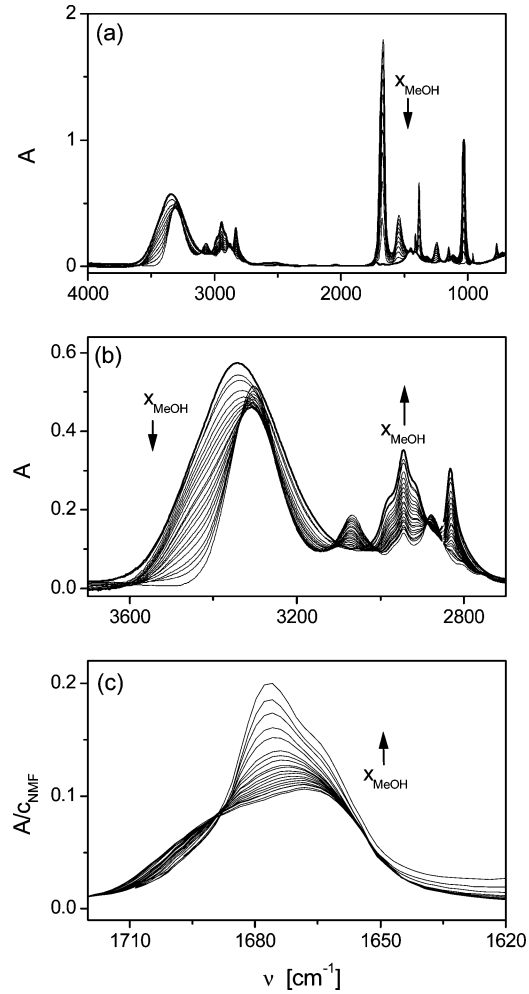

Figure 1. FTIR spectra of NMF−MeOH mixtures for methanol mole fractions varying by 0.05. (a) The whole spectrum in absorbance scale. (b) ν(OH), ν(NH), and ν(CH) bands in absorbance scale. (c) The ν(CO) band of NMF in A/c_{NMF} units: A, ATR-corrected absorbance; c_{NMF}, molar concentration of NMF. Increasing methanol mole fraction is shown by arrows.

The results of the factor analysis applied to the ν(C−O) band revealed three environments for the carbonyl group (Figure 4). Taking into account the positions of their maxima, one can distinguish bulk NMF, NMF in a molecular complex with MeOH, and NMF interacting with bulk MeOH in another way than through hydrogen bonds. The last form of NMF, occurring in a narrow range of mixture composition, was not distinguished by the factor analysis of the whole spectra, as its concentration was expected to be very low (because of the low content of NMF in the system).

The difference-spectra method was applied to the ν(CO) band converted into the molar absorbance of NMF. The derivative of the spectrum at zero molality of MeOH was obtained by approximation of the spectra at any wavenumber from their dependence on the methanol molality in the range of $0 \le x_{MeOH} \le 0.3$ using quadratic regression; $R^2 > 0.999$. This is shown in Figure 5a together with the spectrum of pure NMF decomposed into analytical components. The derivative was then used for calculating the difference spectra according to eq 1 for trial N values; that for $N = 0.55$, containing no more than 0.5% of bulk NMF spectrum, was treated as the "true" MeOH-affected spectrum of NMF (Figure 5b). This value of N means that in an infinitely dilute solution of methanol in NMF one MeOH molecule affects on average 0.55 NMF molecules. As can be

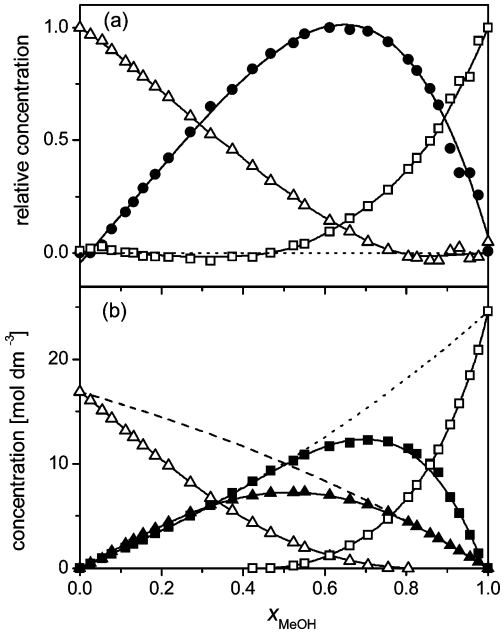

Figure 2. Factor analysis of NMF−MeOH spectra in absorbance scale (4000−700 cm^{-1}). (a) Relative concentrations of different species as a function of methanol mole fraction: NMF nonbonded to MeOH (△); MeOH nonbonded to NMF (□); complex of NMF and MeOH (●). (b) Molar concentrations of nonbonded NMF (△); nonbonded MeOH (□); NMF in a complex with MeOH (▲); MeOH in a complex with NMF (■); total NMF (dashed line); total MeOH (dotted line).

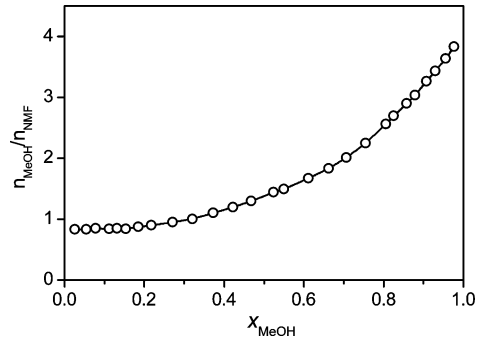

Figure 3. Ratio of NMF and MeOH in the complex depending on methanol mole fraction in the mixtures, determined from the whole spectrum in the absorbance scale.

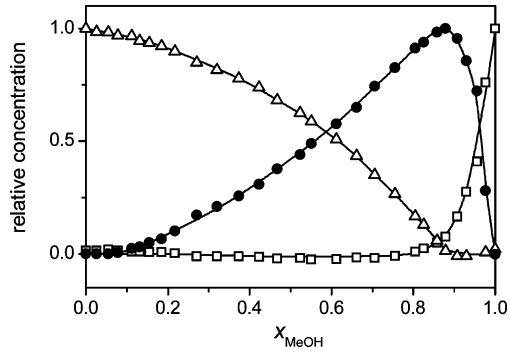

Figure 4. Factor analysis of the ν(CO) band of NMF (1750−1650 cm^{-1}). Relative concentrations of different forms of NMF as a function of methanol mole fraction: NMF nonbonded to MeOH (△); NMF in bulk MeOH (□); NMF in a complex with MeOH (●).

seen from the figure, the affected spectrum consists of two components, revealing two different energetic states of the CO group affected by MeOH molecules in the NMF-rich mixtures.

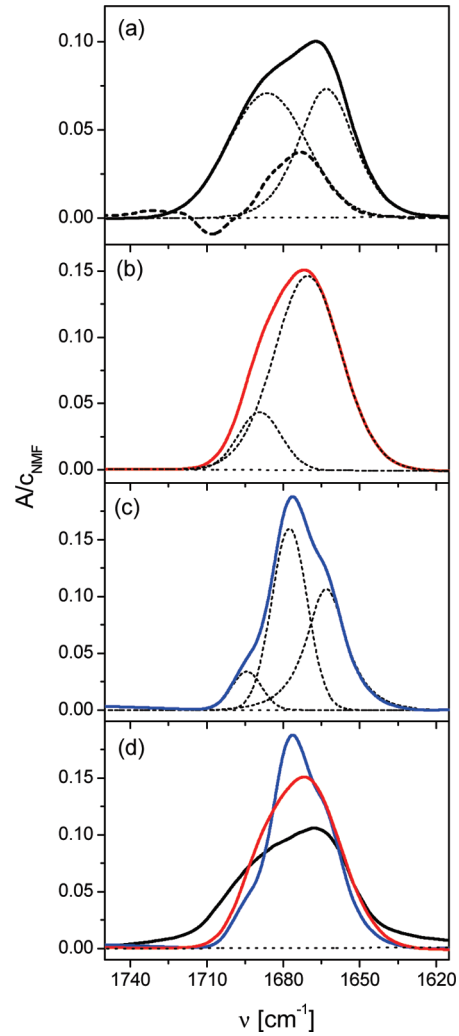

Figure 5. Difference spectra method analysis applied to the ν(CO) band of NMF in the NMF-rich region of the NMF−MeOH mixtures. (a) Decomposition of the bulk NMF spectrum (solid line) into analytical component bands (dotted line) and the derivative ($\delta\varepsilon/\delta m$) for experimental spectra at zero molality of MeOH (dashed line). (b) Decomposition of the MeOH-affected spectrum (solid line) into analytical component bands (dotted line). (c) Decomposition of the NMF spectrum extrapolated to $x_{MeOH} = 1$ (solid line) into analytical component bands (dotted line). (d) The comparison of band shapes for bulk NMF (black), NMF affected by MeOH (red), and NMF extrapolated to $x_{MeOH} = 1$ (blue).

Figure 5c presents the spectrum of NMF extrapolated to $x_{MeOH} = 1$, obtained by approximation of the spectral data at each wavenumber in the range $0.55 \leq x_{MeOH} \leq 0.95$. The absorption change with the mole fraction of methanol was adequately described by a third-order polynomial; $R^2 > 0.999$. Decomposition of this spectrum showed three energetic states of the CO group in MeOH-rich mixtures. In Figure 5d, the shapes and positions of the CO band in different environments are compared.

Ab Initio Results. Geometry optimization was performed for molecular clusters in which all possibilities of bonding between the central NMF molecule and one or more MeOH molecules (or another NMF molecule in a 2:1 complex) were assumed (for simplicity, in this section, complexes of defined stoichiometry will be denoted in a short form as the ratio of NMF to MeOH molecules). The structures for which the geometries were optimized are listed in Tables 1 and 2, classified as those with a *trans*-NMF and those with a *cis*-NMF isomer. They are

TABLE 1: Thermodynamic Functions Calculated for Complexes of *trans*-NMF with MeOH in the Gas Phase

complex	structure	E_0[a]	ΔE_0[b]	ΔG_{298}[c]	$T\Delta S_{298}$[d]
$(t\text{-NMF})_2(\text{MeOH})_1$	A	−534.131351	−51.65	14.88	−59.17
	B	−534.130628	−49.76	18.35	−60.75
	C	−534.130266	−48.81	10.16	−51.02
	D	−534.130121	−48.42	13.72	−54.42
	E	−534.129228	−46.08	13.32	−50.64
$(t\text{-NMF})_1(\text{MeOH})_1$	A	−324.921288	−22.22	12.84	−32.12
	B	−324.921013	−21.50	8.44	−26.46
	C	−324.919967	−18.75	11.48	−26.03
$(t\text{-NMF})_1(\text{MeOH})_2$	A	−440.648008	−55.69	20.36	−72.79
	B	−440.646778	−52.47	23.35	−72.37
	C	−440.643848	−44.77	19.86	−59.36
	D	−440.643593	−44.10	19.24	−57.80
	E	−440.643576	−44.06	22.97	−61.76
	F	−440.642562	−41.40	28.17	−65.12
$(t\text{-NMF})_1(\text{MeOH})_3$	A	−556.377157	−95.54	23.93	−116.21
	B	−556.372815	−84.14	26.33	−105.39
	C	−556.370989	−79.35	35.33	−110.07
	D	−556.369623	−75.76	37.74	−109.07
	E	−556.369035	−74.22	34.62	−103.28
	F	−556.367991	−71.48	36.34	−103.68
	G	−556.367311	−69.69	42.32	−107.08
	H	−556.365856	−65.87	36.49	−95.80
$(t\text{-NMF})_1(\text{MeOH})_4$	A	−672.108568	−141.33	16.62	−154.25
	B	−672.105953	−134.47	25.42	−156.21
	C	−672.105637	−133.64	24.81	−154.55
	D	−672.099390	−117.24	38.16	−150.82
	E	−672.095118	−106.02	37.84	−136.82
	F	−672.094132	−103.43	50.51	−149.10
	G	−672.093518	−101.82	46.06	−141.52
	H	−672.093134	−100.81	51.27	−146.31
	I	−672.091156	−95.62	46.25	−134.93

[a] Total energy, including zero-point vibrational energy (hartree). The values for *trans*-NMF and MeOH molecules are −209.198853 and −115.713971, respectively. [b] Interaction energy at 0 K, calculated as the difference between the energy of a cluster and the sum of energies of the separate component molecules (kJ·mol^{-1}). [c] Gibbs free energy of interactions at 298 K, calculated as the difference between the Gibbs free energy of a cluster and the sum of Gibbs free energies of the component molecules, corrected for the entropy of mixing (kJ·mol^{-1}). [d] Entropy contribution at 298 K, calculated as the difference between the entropy of a cluster and the entropy of the mixture of component molecules (kJ·mol^{-1}). Enthalpies of interactions, ΔH_{298}, also available from *ab initio* calculations, obey the obvious relation $\Delta H_{298} = \Delta G_{298} + T\Delta S_{298}$. The letters describing structures refer to the respective labels in Figure 6 and in figures available as Supporting Information to this paper.

ordered with respect to diminishing absolute values of energies including electronic and zero-point vibrational energies, E_0, within each complex composition. The same sequence of the structures is shown in Figure 6 for the 1:1 complex; the structures for the remaining stoichiometries, because of their great number, are available as Supporting Information. As seen here, two kinds of hydrogen bonds through lone electron pairs of the oxygen atom in the NMF molecule were distinguished: "parallel" and "antiparallel" to the C−H (formyl) bond.

The energies obtained for the optimized structures were used for calculating the interaction energies between molecules, ΔE_0, defined as the difference between the energy of a complex and the sum of the energies of the separate molecules. Gibbs free energy and entropy changes accompanying the formation of individual structures were calculated using the values of the respective functions obtained for the optimized structures and for the component molecules at 298.15 K and 1 atm; the entropies of mixing of the latter were taken into account. All results are presented in Tables 1 and 2.

TABLE 2: Thermodynamic Functions Calculated for Complexes of *cis*-NMF with MeOH in the Gas Phase[a]

complex	structure	E_0	ΔE_0	ΔG_{298}	$T\Delta S_{298}$
$(c\text{-NMF})_2(\text{MeOH})_1$	A	−534.139495	−88.03	−5.43	−78.58
	B	−534.135726	−78.13	0.29	−73.86
$(c\text{-NMF})_1(\text{MeOH})_1$	A	−324.923379	−35.21	5.66	−39.51
	B	−324.919393	−24.74	8.52	−30.36
$(c\text{-NMF})_1(\text{MeOH})_2$	A	−440.653495	−77.60	5.57	−81.86
	B	−440.646641	−59.60	19.24	−76.12
	C	−440.645572	−56.79	18.17	−72.06
$(c\text{-NMF})_1(\text{MeOH})_3$	A	−556.380766	−112.52	8.71	−118.99
	B	−556.376832	−102.19	19.98	−119.74
	C	−556.375618	−99.00	23.05	−119.65
	D	−556.375460	−98.58	18.74	−114.45
	E	−556.374846	−96.97	21.15	−114.79
	F	−556.372672	−91.27	28.32	−116.66
$(c\text{-NMF})_1(\text{MeOH})_4$	A	−672.106396	−143.13	20.66	−161.27
	B	−672.102384	−132.59	21.02	−149.73
	C	−672.102301	−132.38	28.87	−158.24
	D	−672.102276	−132.31	28.85	−158.17
	E	−672.101168	−129.40	27.28	−152.68
	F	−672.100578	−127.85	30.55	−154.81
	G	−672.098550	−122.53	38.95	−158.14
	H	−672.098470	−122.32	33.47	−151.79

[a] The details are the same as those in the footnote for Table 1. The total energy, E_0, calculated for the *cis*-NMF molecule is −209.195998 (hartree).

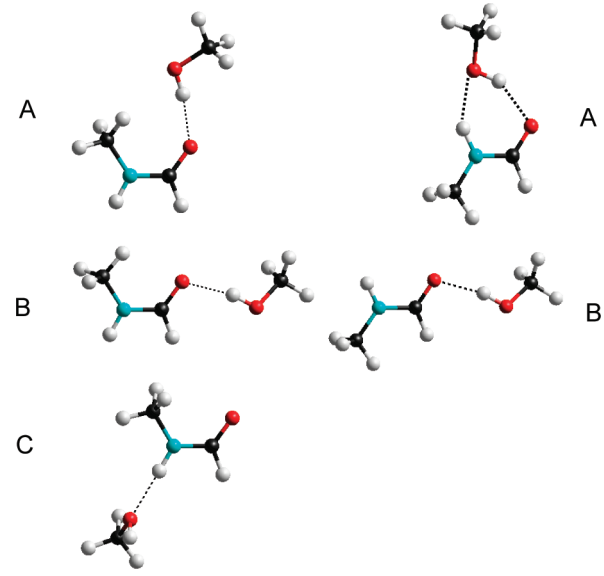

Figure 6. Optimized structures for the $(\text{NMF})_1(\text{MeOH})_1$ complex in the gas phase. Red spheres denote oxygen, gray spheres denote hydrogen, and blue spheres denote nitrogen atoms. Clusters containing *trans*-NMF are on the left side, and those with *cis*-NMF are on the right side. The letters describing the clusters refer to Tables 1 and 2.

Comparison of the ΔE_0 values for complexes of the same stoichiometry shows that intermolecular interactions with a contribution from *cis*-NMF were clearly stronger than those with the *trans* isomer. This evidently resulted from the unique ability of the *cis* isomer to form cyclic structures. Among the complexes formed by the *trans* isomer, the highest interaction energies were found for the structures with chains of two, three, or four MeOH molecules that eventually also led to the cyclic structures.

The ΔG_{298} values for complexes in the gas phase are all positive (with one exception) and increase with the number of MeOH molecules in the complex. Simple calculations indicated that remarkable amounts (at least 1%) of these clusters can be expected in the gas phase at standard conditions for the 2:1, 1:1, and 1:2 complexes formed by *cis*-NMF. Complexes with three and four MeOH molecules are practically nonexistent at these conditions.

TABLE 3: Thermodynamic Functions for Complexes of *trans*-NMF with MeOH in Liquid NMF and Liquid MeOH Calculated in the PCM Model

complex	structure	E_0[a]	ΔE_0[b]	ΔG_{298}[c]	$T\Delta S_{298}$[d]
		liquid NMF			
$(t\text{-NMF})_2(\text{MeOH})_1$	A	−534.158459	−122.83	−55.00	−61.05
	B	−534.157673	−120.76	−42.72	−73.86
	C	−534.158189	−122.12	−46.30	−71.34
	D	−534.157227	−119.59	−50.85	−61.76
	E	−534.157401	−120.05	−43.71	−71.19
$(t\text{-NMF})_1(\text{MeOH})_1$	A	−324.940908	−73.73	−37.46	−33.49
	B	−324.942028	−76.68	−42.88	−30.86
	C	−324.940905	−73.73	−37.14	−33.65
		liquid MeOH			
$(t\text{-NMF})_1(\text{MeOH})_1$	A	−324.940489	−72.63	−36.51	−33.31
	B	−324.941554	−75.43	−38.20	−36.40
	C	−324.940703	−73.20	−34.22	−37.75
$(t\text{-NMF})_1(\text{MeOH})_2$	A	−440.667588	−107.10	−33.08	−72.33
	B	−440.665986	−102.90	−28.66	−70.85
	C	−440.666488	−104.21	−27.31	−74.92
	D	−440.666363	−103.89	−32.14	−69.15
	E	−440.664206	−98.22	−7.48	−94.51
	F	−440.665131	−100.65	−28.89	−67.55
$(t\text{-NMF})_1(\text{MeOH})_3$[e]	A	−556.386613	−120.37	−1.19	−115.66
	B	−556.392050	−134.65	−21.77	−108.64
	D	−556.390830	−131.44	−16.09	−112.57
	E	−556.391157	−132.30	−19.46	−109.58
	F	−556.391450	−133.07	−19.61	−112.15
	G	−556.390392	−130.29	−17.14	−110.40
	H	−556.390291	−130.03	−18.13	−107.98

[a] Total energy, including zero-point vibrational energy (hartree). [b] Interaction energy at 0 K, calculated as the difference between the energy of a cluster in the respective liquid and the sum of energies of the separate component molecules in the gas phase ($kJ \cdot mol^{-1}$). [c] Gibbs free energy of interactions at 298 K, calculated as the difference between the Gibbs free energy of a cluster in the respective liquid and the sum of Gibbs free energies of the component molecules, corrected for the entropy of mixing ($kJ \cdot mol^{-1}$). [d] Entropy contribution at 298 K, calculated as the difference between the entropy of a cluster in the respective liquid and the entropy of the mixture of component molecules ($kJ \cdot mol^{-1}$). [e] Calculations for structure C were not successful.

TABLE 4: Thermodynamic Functions for Complexes of *cis*-NMF with MeOH in Liquid NMF and Liquid MeOH Calculated in the PCM Model[a]

complex	structure	E_0	ΔE_0	ΔG_{298}	$T\Delta S_{298}$
		liquid NMF			
$(c\text{-NMF})_2(\text{MeOH})_1$	A	−534.153646	−125.18	−40.78	−80.60
	B	−534.152848	−123.09	−42.92	−75.68
$(c\text{-NMF})_1(\text{MeOH})_1$	A	−324.935084	−65.94	−22.24	−44.16
	B	−324.940583	−80.38	−44.83	−33.08
		liquid MeOH			
$(c\text{-NMF})_1(\text{MeOH})_1$	A	−324.938571	−75.09	−38.66	−34.04
	B	−324.939754	−78.20	−40.18	−35.81
$(c\text{-NMF})_1(\text{MeOH})_2$	A	−440.663945	−105.03	−19.15	−85.12
	B	−440.665948	−110.29	−31.57	−77.71
	C	−440.663205	−103.09	−25.06	−76.70
$(c\text{-NMF})_1(\text{MeOH})_3$	A	−556.391422	−140.49	−18.04	−120.38
	B	−556.388934	−133.96	−6.40	−127.64
	C	−556.388672	−133.27	−8.04	−124.98
	D	−556.389105	−134.41	−19.37	−112.26
	E	−556.390791	−138.84	−19.75	−115.91
	F	−556.385100	−123.89	−0.48	−122.76

[a] The details are the same as those in the footnote for Table 3.

The structures optimized in the gas phase were subsequently recalculated using the polarizable continuum model (PCM) for liquid NMF and liquid MeOH. Calculations were performed for the complexes that were expected in the extreme regions of mixed solvent composition, that is, for the 2:1 and 1:1 complexes in liquid NMF and for the 1:1, 1:2, and 1:3 complexes in liquid MeOH.

Geometries optimized in the liquid solvents were generally similar to those in the gas phase. In several cases, an opening of the cyclic structure or a bending of the chain of molecules connected to a central NMF molecule occurred. Minor changes consisted of turning external molecules in the complex around the axis of the hydrogen bond. The mostly changed structures are available as Supporting Information together with the respective structures in the gas phase for comparison.

The energies for the structures embedded in a solvent cavity are listed in Tables 3 and 4. They were lower than the respective energies in the gas phase reflecting not only interactions of the clusters with the surrounding solvent but also the changes in interactions inside the cluster when it was transferred from the gas to the liquid phase. Thus, the total interaction energy for a structure placed in the liquid amide or methanol was calculated as the difference between the energy of that structure in the respective liquid solvent and the sum of the energies of the separate component molecules.

Comparison of the data in Tables 3 and 4 shows that the interaction energies of the respective complexes involving *trans*- and *cis*-isomers of NMF were similar in the liquid phase, in contrast to those in the gas phase. Moreover, the differences in energy between the various structures of the same stoichiometry became in most cases less in the liquid than in the gas phase. Obviously, the strong solvation interactions moderate the energetic differences between the clusters to some degree. It should also be noted that the order of energies for different structures in the liquid phase does not agree with that in the gas phase.

The Gibbs free energies and entropies of the formation of complexes from single molecules in liquid amide and methanol were calculated analogously to the energies but regarding the entropies of mixing of the components in the gas phase; the results are listed in Tables 3 and 4. The Gibbs free energy changes were strongly negative, and the relevant equilibrium constants vary from 10^9-10^6 in *N*-methylformamide (for the 2:1 and 1:1 complexes) to 10^5-10^2 in methanol (for the 1:2 and 1:3 complexes).

The ordering of Gibbs free energies for individual structures within the fixed stoichiometry of the complex was not identical with the ordering of their energies (and enthalpies) in the respective liquid phase. In some cases, the greatest stability of the structure resulted from the entropy term. The most stable structures for complexes of various compositions in liquid NMF and liquid MeOH are presented in Figure 7.

For comparison, the thermodynamic functions for $(\text{MeOH})_2$, $(\text{MeOH})_3$, $(\text{NMF})_2$, and $(\text{NMF})_3$ clusters were obtained and are listed in Table 5.

Molecular Complexes in Liquid NMF−MeOH Mixtures in Light of the Experimental and Computational Results. As seen from the factor-analysis results, the mean ratio $n_{\text{MeOH}}/n_{\text{NMF}}$ in the complex increased with increasing methanol content in the mixtures (Figure 3). At the lowest methanol content, the mean number of MeOH molecules for one NMF molecule was about 0.83, remaining less than 1 in the range up to $x_{\text{MeOH}} = 0.3$. This suggests the presence of complexes with at least two amide molecules occurring for each methanol molecule. With the further increase of methanol content in the mixtures, the ratio $n_{\text{MeOH}}/n_{\text{NMF}}$ increased gradually, rising to about 4 at $x_{\text{MeOH}} = 0.976$. It is worth noting that the mean composition of the complex at its maximum concentration ($n_{\text{MeOH}}/n_{\text{NMF}} = 1.76$) is very close to the composition of the mixture ($x_{\text{MeOH}} = 0.64$) (cf. Figures 2a and 3). As the bulk solvents are practically absent

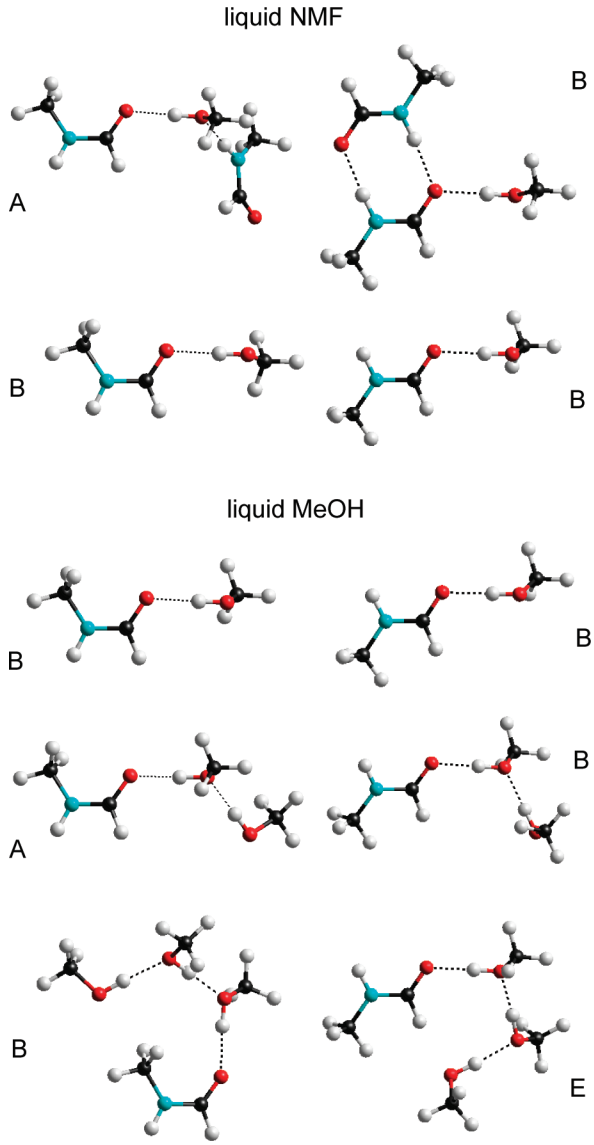

Figure 7. Most stable structures for each stoichiometry of the complexes in both liquid NMF and MeOH. Clusters containing *trans*-NMF are on the left side, and those with *cis*-NMF on the right side. The letters describing the clusters refer to Tables 3 and 4.

at this mole fraction (Figure 2a), the above result of the spectral analysis is in accordance with the main conclusion from the solvation study of the NMF molecule by methanol based on the Kirkwood−Buff theory of solutions and stating that the local mole fractions differ only slightly from the bulk ones.[17,18]

A more detailed discussion of the factor-analysis results is available as Supporting Information to this paper.

High equilibrium constants for complex formation, calculated on the basis of the PCM method in liquid NMF and MeOH, indicated that in the regions of marked excess of one component the other was almost fully complexed. The same can be derived from the factor analysis of the FTIR spectra, presented in Figure 2b. As seen here, the concentration of methanol complexed with NMF was equal to its total concentration in the mixtures up to $x_{MeOH} \approx 0.45$. Similarly, in the mixtures with $x_{MeOH} > 0.8$, the total amount of NMF was bound to MeOH. One may note that the widths of the ranges in which the limiting component is fully complexed are consistent with the values of the equilibrium constants in the respective ranges: those for the 2:1 and 1:1 complexes in the NMF-rich mixtures were on average 4 orders of magnitude higher than those for the 1:2 and 1:3 complexes in the MeOH-rich ones.

TABLE 5: Thermodynamic Functions Calculated for $(MeOH)_2$, $(MeOH)_3$, $(NMF)_2$, and $(NMF)_3$ Complexes

complex	structure	E_0[a]	ΔE_0[b]	ΔG_{298}[c]
		gas phase		
$(MeOH)_2$		−231.434953	−18.41	12.36
$(MeOH)_3$	A	−347.159452	−46.05	24.88
	B	−347.153560	−30.58	31.82
$(t\text{-NMF})_2$	A	−418.406180	−22.25	−0.80
	B	−418.406047	−21.90	14.11
$(t\text{-NMF})_3$	A	−627.616179	−51.51	−1.93
	B	−627.615477	−49.67	−0.54
	C	−627.610190	−35.79	18.29
$(c\text{-NMF})_2$	A	−418.413468	−56.37	−15.11
	B	−418.406210	−37.32	0.60
$(c\text{-NMF})_3$	A	−627.623376	−92.90	−16.61
	B	−627.621367	−87.62	−6.63
	C	−627.614727	−70.19	7.15
		liquid MeOH		
$(MeOH)_2$		−231.449749	−57.25	−22.99
$(MeOH)_3$	A	−347.175562	−88.35	−12.54
	B	−347.172637	−80.67	−6.06
		liquid NMF		
$(t\text{-NMF})_2$	A	−418.432891	−92.38	−63.69
	B	−418.432597	−91.61	−55.16
$(t\text{-NMF})_3$	A	−627.648959	−137.58	−64.84
	B	−627.648541	−136.48	−75.67
	C	−627.647790	−134.51	−65.18
$(c\text{-NMF})_2$	A	−418.427771	−93.93	−53.14
	B	−418.427493	−93.20	−57.16
$(c\text{-NMF})_3$	A	−627.639872	−136.21	−57.80
	B	−627.639942	−136.39	−56.70
	C	−627.640860	−138.80	−66.99

[a] Total energy (hartree). [b] Interaction energy at 0 K ($kJ \cdot mol^{-1}$), defined as in Table 1 for clusters in the gas phase and in Table 3 for clusters in the liquid NMF and MeOH. [c] Gibbs free energy of interactions at 298 K ($kJ \cdot mol^{-1}$), defined as in Table 1 for clusters in the gas phase and in Table 3 for clusters in the liquid NMF and MeOH.

The broad range for the existence of bulk NMF (clearly seen in Figure 2a) suggests that intermolecular interactions between amide molecules are stronger than those between amide and methanol molecules. This idea is supported by the computational results for complexes in the liquid phase: the total interaction energies were distinctly higher for clusters consisting of NMF molecules than for clusters composed of the same number of different molecules. Also, interactions through the carbonyl oxygen of the NMF molecules were on average stronger in bulk NMF than in their complexes with MeOH, as can be seen from the mean positions of the bulk and affected spectra of NMF in the carbonyl-group absorption regions (1668 and 1671 cm^{-1}, respectively).

Analysis of FTIR spectra in the CO stretching region revealed different energetic states of the carbonyl group in the NMF-rich mixtures (the MeOH-affected spectrum) and in the MeOH-rich mixtures (the spectrum extrapolated to $x_{MeOH} = 1$). The positions of the components of the above spectra reflect the strength of the interactions of the carbonyl oxygen with surrounding molecules, with a more red-shifted band indicating stronger interaction. Particular components can be ascribed to complexes of defined stoichiometry in agreement with the expected degree of polarization of the CO group. Two components of the MeOH-affected spectrum (at 1671 and 1691 cm^{-1}) may correspond to $(NMF)_2(MeOH)_1$ and $(NMF)_1(MeOH)_1$ complexes, respectively, according to the factor-analysis results

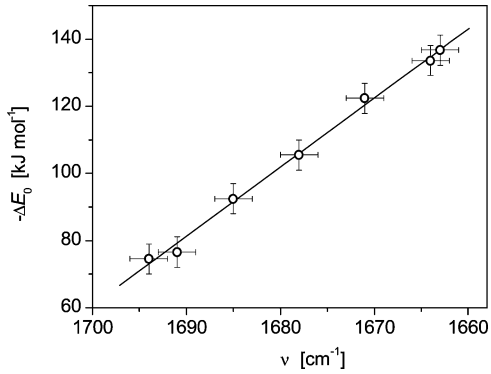

Figure 8. Correlation between the ν(CO) band for different environments of NMF revealed by the analysis of FTIR spectra (values in the text) and the interaction energies of the complexes ascribed to the particular bands, calculated in the PCM model. The energies for *trans*-NMF complexes were taken with the factor 0.9 and those for *cis*-NMF complexes with the factor 0.1, according to the population of both isomers.[9,11,12] Error for the energies was estimated from the regression analysis assuming a wavenumber error of ± 2 cm^{-1}.

discussed above. Two of three components of the NMF spectrum in the MeOH-rich region (at 1664 and 1678 cm^{-1}) were ascribed to $(NMF)_1(MeOH)_3$ and $(NMF)_1(MeOH)_2$ complexes, respectively. Complexes with higher MeOH content were neglected because of their low concentrations, as concluded from the considerable decrease of the absolute values of ΔG_{298} and thus the equilibrium constants for the 1:1, 1:2, and 1:3 complexes (Tables 3 and 4). However, the most blue-shifted component of the NMF spectrum in a methanolic environment (at 1694 cm^{-1}) cannot be unequivocally interpreted. It may represent an $(NMF)_1(MeOH)_1$ complex in a cavity of methanol or NMF molecules interacting nonspecifically with bulk methanol. The first possibility is justified by the results presented in Figure 8 (text below), and the second one corresponds with the factor-analysis results for the CO band in the MeOH-rich mixtures (Figure 4). For two components of the bulk spectrum (at 1663 and 1685 cm^{-1}), $(NMF)_3$ and $(NMF)_2$ clusters, respectively, were assumed to be responsible.

An interesting correlation between the positions of the CO spectra for the above complexes and their total interaction energies calculated in the liquid phase was found. The spectra representing NMF in three environments, bulk, MeOH-affected NMF, and NMF in the MeOH-rich region, were considered. The interaction energies of the complexes were determined from the energies of the individual structures by assuming that each structure contributes to the energy proportionally to its content (see the relevant data in Tables 3−5). A linear correlation ($R^2 = 0.996$) between both quantities was observed (Figure 8). This correlation is similar to that known as the Badger−Bauer rule, stating that the position of the OH stretching band changes proportionally to the energy of a hydrogen bond.[35] The rule has been tested for many donor−acceptor systems[36−39] and used extensively in hydration studies of ionic and nonionic species.[24−28,30−32]

The most probable structures for the complexes of different stoichiometries presented in Figure 7 show clear similarities. The structures are open (the only cyclic structure for the 2:1 complex of *cis*-NMF does not contain a MeOH molecule in the ring), and in all of them, the MeOH molecule interacts with the carbonyl oxygen of the NMF molecule. The second and third MeOH molecules form a chain. With one exception, the structures exhibit the same pattern of hydrogen bonding between carbonyl oxygen and hydroxyl hydrogen: it is directed "parallel" to the C−H (formyl) bond. The exception concerns the 1:3 cluster of the *trans* isomer, in which the H-bond between NMF and MeOH molecules is "antiparallel" to the C−H (formyl) bond. It may be noted that methanolic chains in both structures of the 1:3 complex form similar configurations with the methyl group of the NMF molecule; the effect is better visualized in the three-dimensional models of these structures.

Obviously, structures other than those considered above are also present in solutions, especially when equilibrium constants between the first and succeeding structures do not differ markedly. This concerns particularly the 1:2 complexes of *trans*-NMF and the 1:3 complexes of *cis*-NMF in the MeOH-rich mixtures.

It should be added that results referring to *cis*-NMF have less significance because of the low population of this isomer in the real liquid: it varies from 5 to 18% according to a previous study.[9,11,12]

What Can Be Learned from FTIR Spectra about Molecular Complexes? As we have previously performed the analysis of FTIR spectra as presented in this study for analogous systems (DMF−MeOH and FA−MeOH),[1,2] we are able to summarize the advantages of applying the factor analysis and the difference spectra method to the spectra of liquid binary mixtures.

First, we found that the composition of a complex revealed by the factor analysis was not constant over the range of its occurrence but changed gradually with the mixed solvent composition. This fact allowed us to assume that such a complex actually corresponds to a set of clusters in equilibrium which is shifted with the composition of the mixtures. Accompanying changes in polarization of that averaged individual are also gradual; therefore, the complex is represented by a single factor in the spectral analysis. This interpretation was fully confirmed by the results of the difference spectra method but stands in opposition to the commonly accepted understanding of the results of chemometric methods.

The most striking difference between the three systems was the number of amide−methanol complexes obtained by the factor analysis: one complex in the DMF−MeOH and NMF−MeOH mixtures and two complexes in the FA−MeOH mixtures. Our explanation is that the main criterion of distinguishing individual complexes by the factor analysis is the manner of polarization of amide molecules in the complex. DMF molecules can interact with methanol molecules only through the carbonyl oxygen; this is the most probable option also for NMF molecules (as can be seen from *ab initio* results for liquid phases). In contrast, FA molecules use all sites for binding methanol molecules with comparable probability so their polarization in clusters with two and more methanol molecules may differ considerably from that in clusters with one methanol molecule.

Applying the factor analysis to the absorption of groups directly participating in the complex formation resulted in the recognition of new individuals, not detected by the whole-spectrum analysis because of their low concentrations and narrow ranges of occurrence. In such a manner, DMF, NMF, and FA molecules interacting with bulk methanol by disturbing its structure without forming hydrogen bonds were found as well as MeOH molecules interacting nonspecifically with bulk DMF.

Analysis by the difference spectra method revealed various energetic states of the component in excess (amide in all cases and methanol in the DMF−MeOH system), which were then attributed to the probable structures of the complexes. The assignment was based on the position of the components of the affected spectrum and thus on the interaction energies in

the complex. In this way, one can distinguish between the complexes having interactions both stronger and weaker than those in the bulk solvent and also recognize the much weaker nonspecific interactions mentioned above.

Parallel analysis of the absorption of the groups taking part in hydrogen bonding from both molecules allows for a cross-checking of results, enhancing their reliability. Unfortunately, this was achievable only for the ν(CO) and ν(OH) bands in the DMF−MeOH mixtures, due to the overlap of the O−H, N−H, and C−H absorptions in the remaining cases. Owing to this possibility, the weak hydrogen bonds formed by formyl and methyl protons are postulated in the DMF−MeOH system.

Conclusions

Molecular interactions in the NMF−MeOH system have been described using the advantageous combination of experimental and theoretical research. Although the factor analysis of FTIR spectra is a sensitive method for recognizing even weak intermolecular interactions, its results are difficult to explain unambiguously without the help of other methods. In our study, the extensive information on molecular complexes was drawn by comparison of the factor-analysis results with those of the difference spectra method. The interpretation of the spectral data was enhanced by the structural and energetic characteristics of the complexes supplied by *ab initio* calculations. Thermodynamic functions calculated for the optimized structures allowed us to compare them with respect to the interaction energies within a fixed stoichiometry as well as to select the most stable structures in the liquid phase. Thus, the proposed method for studying binary liquids provides a comprehensive picture of intermolecular interactions obtained by a cooperation of complementary methods that contribute to the increased understanding of their self-consistent results.

Thermodynamic characteristics obtained for the complexes in the liquid phase using PCM approximation seem to be well established for two reasons. First, the most stable structures for different stoichiometries showed an astonishing regularity (when one takes into account a variety of optimized clusters) and, second, because there is a linear correlation found between the interaction energies of the complexes and the positions of the CO stretching vibration bands revealed by the difference spectra method. This correlation suggests that a Badger−Bauer-type rule may be extended to groups that are able to act as proton acceptors in a hydrogen bond system, such as the carbonyl groups of simple amides.

Acknowledgment. This work was supported by internal grants from the Gdańsk University of Technology. Calculations were carried out at the Academic Computer Center in Gdańsk (TASK).

Supporting Information Available: Gas phase optimized structures of $(NMF)_2(MeOH)_1$, $(NMF)_1(MeOH)_2$, $(NMF)_1(MeOH)_3$, and $(NMF)_1(MeOH)_4$ complexes, including *trans* and *cis* isomers; structures in the liquid phases which are mostly changed compared to the respective structures in the gas phase; a detailed discussion of the factor-analysis results. This material is available free of charge via the Internet at http://pubs.acs.org.

References and Notes

(1) Stangret, J.; Kamieńska-Piotrowicz, E.; Szymańska-Cybulska, J. *Spectrochim. Acta, Part A* **2005**, *61*, 3043.
(2) Stangret, J.; Kamieńska-Piotrowicz, E.; Laskowska, K. *Vib. Spectrosc.* **2007**, *44*, 324.
(3) Malinowski, E. R. *Factor Analysis in Chemistry*; John Wiley and Sons: New York, 2002.
(4) Stangret, J. *Spectrosc. Lett.* **1988**, *21*, 369.
(5) Bartel, J.; Buchner, R.; Wurm, B. *J. Mol. Liq.* **2002**, *98−99*, 51.
(6) Hammami, F.; Nasr, S.; Oumezzine, M.; Cortès, R. *Biomol. Eng.* **2002**, *19*, 201.
(7) Skarmoutsos, I.; Samios, J. *Chem. Phys. Lett.* **2004**, *384*, 108.
(8) Tan, H.; Qu, W.; Chen, G.; Liu, R. *J. Phys. Chem. A* **2005**, *109*, 6303.
(9) (a) Martínez, A. G.; Teso Vilar, E.; Garcia Fraile, A.; Martínez-Ruiz, P. *J. Phys. Chem. A* **2002**, *106*, 4942. (b) Martínez, A. G.; Teso Vilar, E.; García Fraile, A.; Martínez-Ruiz, P. *J. Chem. Phys.* **2006**, *124*, 234305.
(10) Cordeiro, J. M. M.; Cordeiro, M. M. A.; Bôsso, A. R. S. A.; Politi, J. R. S. *Chem. Phys. Lett.* **2006**, *423*, 67.
(11) Shin, S.; Kurawaki, A.; Hamada, Y.; Shinya, K.; Ohno, K.; Tohara, A.; Sato, M. *J. Mol. Struct.* **2006**, *791*, 30.
(12) Albrecht, M.; Rice, C. A.; Suhm, M. A. *J. Phys. Chem. A* **2008**, *112*, 7530.
(13) Pikkarainen, L. *Thermochim. Acta* **1991**, *178*, 311.
(14) Zielkiewicz, J. *J. Chem. Thermodyn.* **1995**, *27*, 1275.
(15) Zielkiewicz, J. *J. Chem. Thermodyn.* **1996**, *28*, 887.
(16) Zielkiewicz, J. *J. Chem. Eng. Data* **1998**, *43*, 650.
(17) Zielkiewicz, J. *J. Chem. Soc., Faraday Trans.* **1998**, *94*, 1713.
(18) Zielkiewicz, J. *Phys. Chem. Chem. Phys.* **2000**, *2*, 2925.
(19) Eaton, G.; Symons, M. C. R.; Rastogi, P. P. *J. Chem. Soc., Faraday Trans. 1* **1989**, *85*, 3257.
(20) Gerothanassis, I. P.; Vakka, C. *J. Org. Chem.* **1994**, *59*, 2341.
(21) Díez, E.; San Fabian, J.; Gerothanassis, I. P.; Esteban, A. L.; Abboud, J-L. M.; Contreras, R. H.; de Kowalewski, D. G. *J. Magn. Reson.* **1997**, *124*, 8.
(22) de Kowalewski, D. G.; Kowalewski, V. J.; Contreras, R. H.; Díez, E.; Casanueva, J.; San Fabian, J.; Esteban, A. L.; Galache, M. P. *J. Magn. Reson.* **2001**, *148*, 1.
(23) Cossi, M.; Crescenzi, O. *Theor. Chem. Acc.* **2004**, *111*, 162.
(24) Stangret, J.; Gampe, T. *J. Phys. Chem. B* **1999**, *103*, 3778.
(25) Stangret, J.; Kamieńska-Piotrowicz, E. *J. Chem. Soc., Faraday Trans.* **1997**, *93*, 3463.
(26) Stangret, J.; Gampe, T. *J. Phys. Chem. A* **2002**, *106*, 5393.
(27) (a) Śmiechowski, M.; Stangret, J. *J. Chem. Phys.* **2006**, *125*, 204508. Śmiechowski, M.; Stangret, J. *J. Phys. Chem. A* **2007**, *111*, 2889.
(28) Gojło, E.; Śmiechowski, M.; Panuszko, A.; Stangret, J. *J. Phys. Chem. B* **2009**, *113*, 8128.
(29) Kamieńska-Piotrowicz, E.; Stangret, J.; Szymańska-Cybulska, J. *Spectrochim. Acta, Part A* **2007**, *66*, 1.
(30) Gojło, E.; Gampe, T.; Krakowiak, J.; Stangret, J. *J. Phys. Chem. A* **2007**, *111*, 1827.
(31) Panuszko, A.; Gojło, E.; Zielkiewicz, J.; Śmiechowski, M.; Krakowiak, J.; Stangret, J. *J. Phys. Chem. B* **2008**, *112*, 2483.
(32) Panuszko, A.; Bruździak, P.; Zielkiewicz, J.; Wyrzykowski, D.; Stangret, J. *J. Phys. Chem. B* **2009**, *113*, 14797.
(33) Zhao, Z.; Malinowski, E. R. *Anal. Chem.* **1999**, *71*, 602.
(34) Frisch, M. J.; Trucks, G. W.; Schlegel, H. B.; Scuseria, G. E.; Robb, M. A.; Cheeseman, J. R.; Montgomery, J. A., Jr.; Vreven, T.; Kudin, K. N.; Burant, J. C.; Millam, J. M.; Iyengar, S. S.; Tomasi, J.; Barone, V.; Mennucci, B.; Cossi, M.; Scalmani, G.; Rega, N.; Petersson, G. A.; Nakatsuji, H.; Hada, M.; Ehara, M.; Toyota, K.; Fukuda, R.; Hasegawa, J.; Ishida, M.; Nakajima, T.; Honda, Y.; Kitao, O.; Nakai, I.; Klene, M.; Li, X.; Knox, J. E.; Hratchian, H. P.; Cross, J. B.; Bakken, V.; Adamo, C.; Jaramillo, J.; Gomperts, R.; Stratmann, R. E.; Yazyev, O.; Austin, A. J.; Cammi, R.; Pomelli, C.; Ochterski, J. W.; Atala, P. Y.; Morokuma, K.; Voth, G. A.; Salvador, P.; Dannenberg, J. J.; Zakrzewski, V. G.; Dapprich, S.; Daniels, A. D.; Strain, M. C.; Farkas, O.; Malick, D. K.; Rabuck, A. D.; Raghavachari, K.; Foresman, J. B.; Ortiz, J. V.; Cui, Q.; Babul, A. G.; Clifford, S.; Cioslowski, J.; Stefanov, B. B.; Liu, G.; Liashenko, A.; Piskorz, P.; Komaromi, I.; Martin, R. L.; Fox, D. J.; Keith, T.; Al-Laham, M. A.; Peng, C. Y.; Nanayakkara, A.; Challacombe, M.; Gill, P. M. W.; Johnson, B.; Chen, W.; Wong, M. W.; Gonzalez, C.; Pople, J. A. *Gaussian 03*, revision B.05; Gaussian, Inc.: Wallingford, CT, 2004.
(35) Badger, R. M.; Bauer, S. H. *J. Chem. Phys.* **1937**, *5*, 839.
(36) Drago, R. S.; O'Bryan, N.; Vogel, G. C. *J. Am. Chem. Soc.* **1970**, *92*, 3924.
(37) Rao, C. N. R.; Dwivedi, P. C.; Ratajczak, H.; Orville-Thomas, W. J. *J. Chem. Soc., Faraday Trans. 2* **1975**, *71*, 955.
(38) Luck, W. A. P.; Wess, T. *Can. J. Chem.* **1991**, *69*, 1819.
(39) Bricknell, B. C.; Ford, T. A.; Letcher, T. M. *Spectrochim. Acta, Part A* **1997**, *53*, 299.

JP911530D